3D MODELING OF THERMOCHEMICAL ABLATION IN CARBON-BASED MATERIALS: EFFECT OF ANISOTROPY ON SURFACE ROUGHNESS ONSET

Jean Lachaud, Yvan Aspa, Gérard Vignoles, and Jean-Marc Goyhénèche

Laboratoire des Composites ThermoStructuraux (LCTS),
UMR 5801: CNRS-SAFRAN-CEA-UB1,
Domaine Universitaire de Bordeaux – 3, Allée de La Boétie, 33600 Pessac, France
Corresponding author : jean.lachaud@gadz.org

ABSTRACT

Ablation modeling is addressed from the material point of view. Multi-scale surface roughness of two ablated carbon-based materials is first analyzed by SEM and micro-tomography. Then, a 3D reaction-diffusion model is set up and solved to explain the observed morphologies at micrometer scale. To take into account the complex crystalline structure of graphite, the model has been enriched by incorporation of an anisotropic heterogeneous reactivity. The models are solved either analytically or using a homemade simulation code. Results are in correct agreement with observations. This approach contributes to the understanding of the physico-chemical coupled phenomena involved in ablation and of the material intrinsic behavior.

Key words: Degradation models, Environment effects, Ablation modeling, Spacecraft materials, Carbon-based materials.

1. INTRODUCTION

Spatial vehicles often encounter severe environments during atmospheric crossing. Since the speed can reach many km/s in dense atmosphere, the flow close to the nosetip can be hypersonic. In this case a thin bow shock surrounds an inviscid flow (eulerian flow), while a dynamic boundary layer develops in the vicinity of the wall [1]. Typically, temperature of the flow may reach $7000\,K$ and it may lead to a maximal wall temperature of $4500\,K$ for pressures higher than $100\,bar$ [2]. For such an environment, the design of thermal protection systems relies on Carbon/Carbon (C/C) composites, which possess the best compromise between thermal, thermo-chemical and mechanical properties [3]. However, a high interfacial mass transfer, strongly coupled with boundary layer transfer phenomena, leads to surface recession. Indeed, C/C composites are progressively destroyed by oxidation, sublimation and, up to a certain extent, mechanical erosion. These physico-chemical phenomena, collected the term *ablation*, are globally endothermic. Hence they reduce the wall temperature and the heat flux that penetrates the internal structure [2].

Ablation of C/C composites leads to a typical surface roughness which induces an enhancement of heat and mass transfer between the protection wall and the surrounding environment via two major phenomena: (i) it increases the chemically active surface of the wall; (ii) it contributes to the laminar-to-turbulent transition in the dynamic boundary layer. PANT program results shows that the heat flux may be multiplied by a factor up to three in turbulent regime [4]. The obvious consequence is a considerable enhancement of global ablation velocity.

If general phenomenological tendencies are now well explained and simulated in the bulk fluid phase [1, 5], the understanding of the interaction between the material and the flow close to the wall has to be improved. In this work, the emphasis is set on surface roughness analysis and modeling for two carbon-based materials: a carbon/carbon composite (C/C) and a poly-crystalline graphite. First, the link between the structure of turbostratic carbons and the ablation behavior of carbon-based material is discussed. Second, a morphological analysis of multi-scale roughness features is briefly presented for these two materials. Then, a reaction-diffusion model, set up to explain microscopic roughness lying on C/C, and the arising results are summarized. To model efficiently the surface evolution of the poly-crystalline graphite, the crystalline structure is included in the model through an orientation-dependant gasification rate.

2. LINK BETWEEN TURBOSTRATIC CARBONS STRUCTURE AND THE ABLATION BEHAVIOR OF CARBON-BASED MATERIALS

The constituents of ablative carbon-based materials are made of various kinds of turbostratic carbons [6], which differ from graphite by a less organized and extended crystalline structure [7] (see figure 1). At atomic scale, this difference arises from a lack of pure sp^2 carbon

atoms, as compared to graphite; this fact might be explained by the presence of sp^3-like defects [8]. sp^3-like defects tends to disorientate graphene planes inside graphene layers, which can be slightly curved [8] or exhibit an inter-plane average length up to ten percent larger than graphite one [6]. The change of inter-plane average length (X-diffraction measurement of d_{002}) reduces the local density. d_{002} generally decreases with graphitization degree [9]. The graphene planes extension and the graphene stacks size increase with graphitization degree [7, 9]. Consequently, the local density increase with graphitization degree [6]. The way the graphene stacks are connected together has also a strong effect on density, as it can lead to a more or less optimized space occupation. Then, the size of the representative elementary volume for the global density evaluation is about ten times the size of individual graphene stacks.

The gasification rates (oxidation or sublimation) of the graphene planes increase with plane perimeter to plane surface ratio [10]. Indeed, the reactivity of the edges, whose atoms conformations constitute active sites [11], is three orders of magnitude higher than the reactivity of the surface [12], which contains few defects and then few active sites. (In this work, this effect of the defects on reactivity is not modeled: it is the field of study of *ab initio* calculus or, up to a point, molecular dynamics simulations [13].) It arises the gasification properties of turbostratic carbons are strengthened with the graphitization rate [3], as graphitization tends to expand the graphene planes. Consequently, the gasification rate of turbostratic carbons generally decreases as local density increases [14].

The local recession velocity of the surface depends on the local reactivity. This effect leads to the establishment of surface roughness on composite materials, which are heterogeneous materials made of several kinds of turbostratic carbons. This phenomenon can be balanced by a mass transfer limitation in the fluid phase. This competition between mass transfer and heterogeneous reaction can explain a large part of the roughness features observed on the material surface. In some cases, especially when surface roughness size is of the order of magnitude of the graphene plane, the crystalline structure has to be included in the model through an anisotropic gasification rate.

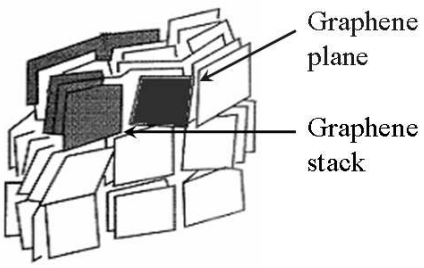

Figure 1. Sketch of the structure of turbostratic carbon [7].

3. ANALYSIS OF SURFACE ROUGHNESS

3.1. C/C analysis

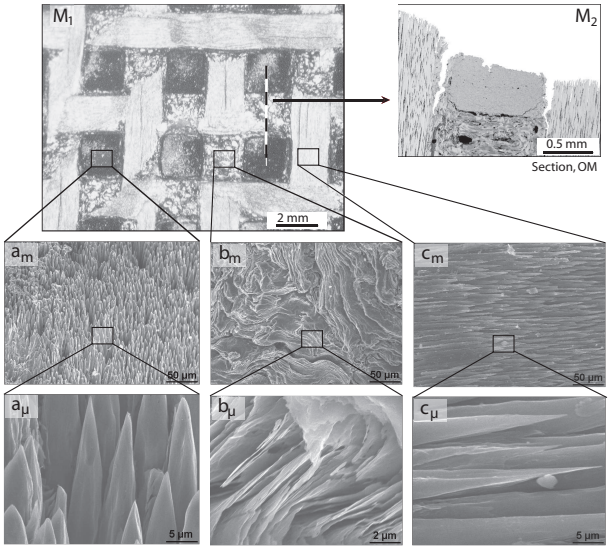

Figure 2. SEM micrographs of 3D C/C surface after plasma jet ablation

C/C composite samples, made from a 3D ex-PAN carbon fiber woven preform and a pitch-based carbon matrix, have been submitted to arc-jet ground tests in stagnation point configuration. The material temperature was high enough ($3000\ K$) to enable both oxidation and sublimation. However, the efficient C/C architecture prevents the sample from being notably eroded during ablation. Surface roughness has mainly been observed by optical microscope (OM), scanning electron microscopy (SEM) and phase-contrast X-ray microtomography (CMT). Let us briefly depict the micrographs of figure 2 which feature the multi-scale surface roughness [15]:

- A macroscopic (M) surface roughness takes place on the lattice of the composite (micrograph M_1). It seems to result from the difference of reactivity between bundles and extra-bundle pitch-based matrix. Notches appear between emerging bundles (micrograph M_2). The section of emerging bundles (tangent or perpendicular to surface) is slightly undulating (micrograph M_2). Indeed, if edges of initially square section of bundles are emerging, creating crenel-like features, they are smoothed out to a wavy form by ablation. Mechanical erosion sporadically occurs through the detachment of an extra-bundle matrix octet.

- A mesoscopic (m) surface roughness develops at the end of emerging bundles, and looks like "needle clusters" (micrograph a_m) -resp. "needle layers" (micrograph c_m)- for bundles perpendicular -resp. parallel- to material surface. In the litera-

ture, many micrographs show such roughness features on carbon-based composites during ablation by oxidation [16, 17] or both oxidation and sublimation [18, 19, 20]. Due to an important recession of the intrabundle matrix, fibers, which are less reactive, are partially stripped, become thinner, and acquire a needle shape. As shown on figure b_m, the surface roughness of the extrabundle pitchbased matrix can be neglected at this scale.

- A microscopic (μ) surface roughness appears on the fibers and on the extra-bundle matrix. Fiber tips are faceted (micrograph a_μ and c_μ). The extrabundle pitch-based matrix shows denuded graphene layers arranged in parallel (micrograph b_μ). It is relevant to its pseudo-crystalline structure.

3.2. Graphite analysis

The studied poly-crystalline graphite, named EDM3, is an isostatic graphite made by Poco Inc. To reduce the residual porosity, the material is impregnated with pitch, which is then carbonized and graphitized. The grain size distribution approximatively obeys a gaussian law with a mean value of $4\,\mu m$ and a standard deviation of $1\,\mu m$. The density value is 1.78 [21]. This material has been submitted to plasma jet ablation [2, 21] and to an oxidation test (this work). The surfaces roughnesses resulting from the two processes are not distinguishable at microscopic and mesoscopic scales. At macroscopic scale, erosion can occur with plasma jet facilities. X-ray computed microtomography has been carried out on EDM3 after the oxidation test (dry air at atmospheric pressure at 625°C). The tomography has been done at ESRF (European Radiation Synchrotron Facilities) in Grenoble (France) on a coherent X-ray source of $100\,\mu m$ wave-length. The resolution is $0.3\,\mu m$. This study reveals the complex multiscale three-dimensional structure of EDM3:

- A macroscopic porosity, visible on the left hand side of the microtomograph (figure 3), is likely to arise from macro-pores poorly filled by the pitch matrix. The diameter of these pores is around $10\,\mu m$. Consequently, they lead to a macroscopic surface roughness when they are opened by ablation. The mark of a macro-pore, which has been uncovered by ablation, can be observed on the surface of the front corner of the tomograph.

- A mesoscopic surface roughness is shown on SEM micrographs of figure 3. It arises from the difference of reactivity between the grains according to their orientation to surface. The more parallel (resp. perpendicular) to surface the graphene planes are, the more resistant (resp. weak) the grains are. This surface roughness size is of the order of the grain size. Moreover, the pitch-based matrix seems to have a higher oxidation rate, as it is not observed on the micrographs.

- At microscopic scale, a lamellar surface roughness appears on the grains (bottom micrograph of figure 3). It has to be correlated to the lamellar structure of the grains.

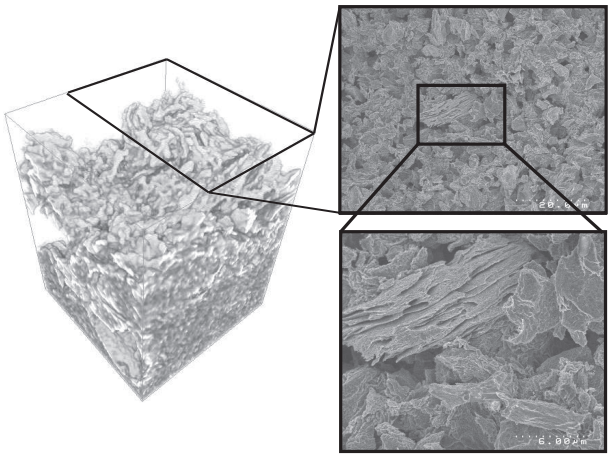

Figure 3. X-ray microtomograph (left) and SEM micrographs (right) of EDM3 graphite surface after ablation

3.3. Synthesis

From the above presented descriptions and classifications, it appears that ablation-related geometrical features of the rough surface mainly follow the material structure. Accordingly, it will be called structural roughness to make a difference with a purely physical roughness which has already been observed on homogeneous materials and modeled [2]. This physical roughness consists in scalloped morphologies and is not correlated to material structure [22]. The cause seems to be a dynamical effect based on the concurrence between bulk transfer and heterogeneous transfer, be it of mass or heat. In addition to such a competition, possible physical phenomena leading to structural roughness appear to be reactivity differences between phases. As a result, models including structure and physics have to be taken in consideration. Moreover, to model accurately poly-cristalline graphite behavior, the material anisotropy has to be taken into account.

4. MODELING OF MESO-SCALE SURFACE ROUGHNESS

4.1. Heterogeneous isotropic materials : C/C composites bundles

The evolution described in section 3.1 of the pointed fibers has been sketched in 2D by Han[19]. We recently succeeded in modeling it in transient regime and to solve it using a simulation code [15]. The model has

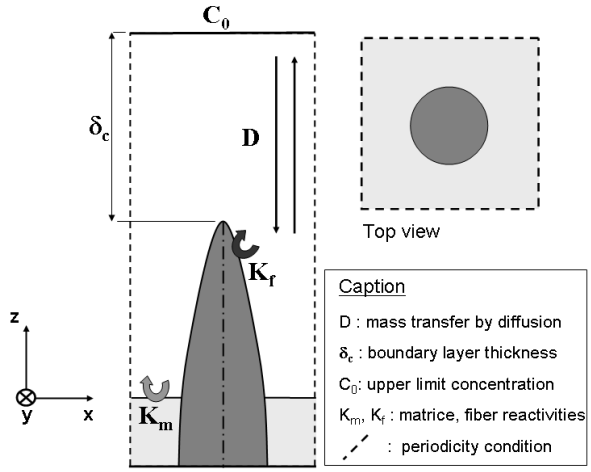

Figure 4. Scheme of the elementary pattern and of the proposed model

been solved analytically in steady state [23]. Let us summarize the hypothesis and the results of these works, as they constitute the physical basis of the model of the following part.

As specified in the previous section, the C/C composite bundles are heterogeneous. They are made of fibers and matrix, which assumed homogeneous and isotropic. They are ablated following either a first order oxidation process or sublimation under Knudsen-Langmuir hypotheses. These two cases are mathematically equivalent considering either reactant diffusion to the wall or vaporized carbon diffusion from the wall [2]. The gasification rate of the fibers (k_f) is lower than for the matrix (k_m).

The proposed model is sketched on figure 4. On this scheme the stationary rough surface is represented; however at initial time, the fluid/solid interface is flat. This profile has therefore to be obtained using a moving fluid/solid interface modeling.

Let us write mass conservation of the reactant (of molar concentration C) in the fluid phase:

$$\frac{\partial C}{\partial t} + \nabla \cdot (-D \nabla C) \; = \; 0 \tag{1}$$

Boundary conditions relative to the model domain are:

- On boundary layer top: $C \; = \; C_0$;
- At the fluid/solid interface the oxidation molar rate r writes:

$$r = (-D \nabla C) \cdot \mathbf{n} \; = \; -k_j C \tag{2}$$

  where $\mathbf{n}$ is the normal to the surface, and k_j (m/s) the reaction kinetic constant of matrix ($j \; = \; m$) or fibers ($j \; = \; f$);

- Periodicity on the lateral boundaries (the bundle section is supposed infinite in transverse directions).

The interface position ($S(x, y, z, t)$) is given by the simultaneous resolution of equations (1-2) and of [2]:

$$\frac{\partial S}{\partial t} \; + \; \mathbf{v} \cdot \nabla S = 0 \tag{3}$$

where $\mathbf{v} \; = \; v_s r \mathbf{n}$ is the surface local normal velocity , with v_s the solid molar volume.

The resolution of this model in steady state for an axisymmetric fiber gives the geometry of the fiber after ablation as a function of two dimensionless numbers (figure 5): (i) the Sherwood number ($Sh \; = \; R_f k_f / D$), which is relevant of reaction versus diffusion competition, (ii) the reactivity contrast between matrix and fibers ($A \; = \; \frac{k_m v_m}{k_f v_f}$) [23]. The model has been validated using independent feeding and validation data [24, 23]. The comparison of the micrographs of figure 2 to the results of the model (figure 5) shows that the Sherwood number is low for the plasma jet test, as fibers are conical. This means that ablation is limited by reaction.

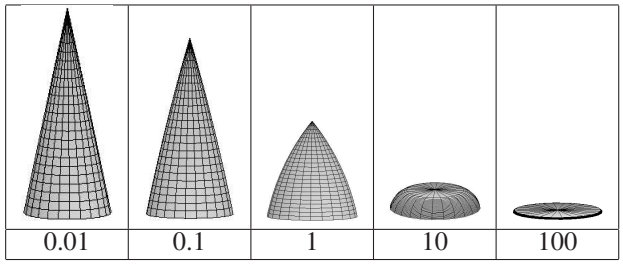

Figure 5. Fiber morphology at steady state as a function of Sh (with $A = 5$).

4.2. Anisotropic materials : EDM3 and C/C composite inter-bundle matrix

As introduced in section 2, the turbostratic carbons possess a complex multi-scale structure. EDM3 has been first tackled in this work due to its repetitive structure and to the direct equivalence between graphene stacks and grains (see subsection 4.2.3). The C/C composite inter-bundle matrix shows an anisotropic structure leading to a microscopic surface roughness (figure 2) which is of interest; unfortunately, its structure is quite complex and irregular. Nevertheless, the results of this section could be applied to the matrix modeling.

First the graphene plane is analyzed, then, two successive changes of scales are done.

4.2.1. Interpretation of the graphene plane reactivity

The starting point of the modeling is the graphene plane. For the materials of the study, the graphene plane cur-

vature is negligible since either the turbostratic carbons possess few defects (poly-crystalline graphite case) or the extension of the graphene planes is small (C/C case) [6]. Graphene edge reactivity is known to be about three order of magnitude larger than in the perpendicular direction (see section 2). A sticking probability is then assigned to the perpendicular direction, noted $P_\perp$, and one to the edge, noted $P_\parallel$ (figure 6). This property can be modeled by an orthotropic sticking probability. Using the notations of the figure 6 it writes:

$$\underline{\underline{P}} = \begin{pmatrix} P_\parallel & 0 & 0 \\ 0 & P_\parallel & 0 \\ 0 & 0 & P_\perp \end{pmatrix}_{(\mathbf{i},\mathbf{j},\mathbf{k})}$$

The interface of a graphene stack is made of a series of surfaces alternately parallel ($S_\parallel$ with a sticking event probability $P_\parallel$) and perpendicular ($S_\perp$ with a sticking probability $P_\perp$) to the graphene plane (figure 6). Let us assume that the average sticking probability, noted $\tilde{P}$, is the arithmetic average of $P_\parallel$ and $P_\perp$ with respect to their real surfaces to effective surface ratio. Let θ be the angle between the normal $\mathbf{n}$ to the material effective surface and $\mathbf{k}$, the local orientation of graphene planes (figure 6). The sticking probability, which can be regarded as a projection of $\underline{\underline{P}}$ on the effective surface, is then a function of θ:

$$\tilde{P}_\theta = \frac{P_\parallel |\sin\theta| + P_\perp |\cos\theta|}{|\sin\theta| + |\cos\theta|} \qquad (4)$$

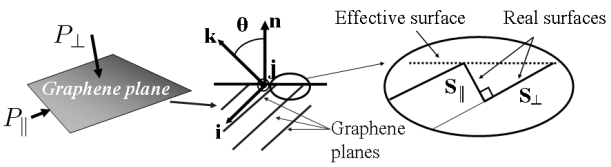

Figure 6. Sketches and notations for the interpretation of graphene plane reactivity

4.2.2. First change of scale: graphene plane to graphene stack

The change of scale is numerical. Indeed, one has to model the complex behavior of a reactive crystalline material. As introduced in section 2 and represented on figure 7, the graphene stack is considered as a perfect lamellar crystallite, constituted of flat graphene planes. Under these hypotheses, the graphene stack retains the orthotropic property of graphene planes. Consequently, the direction $\mathbf{k}$ fully describes the stack orientation. The surface reactivity is a function of graphene stack orientation compared to the interface orientation. Let be α the angle between $\mathbf{k}$ and $\mathbf{n}$. Note that for rough surfaces α is different from θ, as θ is affected by a local orientation, while α arises from a global interface orientation.

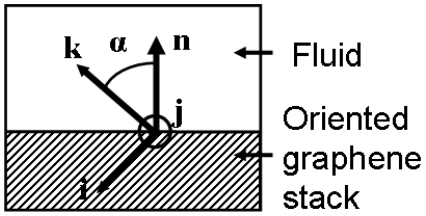

Figure 7. Sketches and notations for graphene stack modeling

To solve this problem in 3-D and in non-stationary regime, an efficient numerical simulation code, named AMA, has been developed on a Monte-Carlo random-walk principle. AMA, which is a C ANSI implementation, contains five main parts. (i) A 3-D image containing several phases (fluid/solids) is described by discrete cubic voxels method. (ii) The moving fluid/solid interface is determined by a simplified marching cube approach [25]. (iii) Mass transfer by diffusion is simulated by a Brownian motion simulation technique [26], which is a continuum (grid-free) and rapidly converging method to simulate diffusion in a continuous fluid. (iv) Heterogeneous anisotropic first-order reaction on the wall is simulated by a sticking probability ($\tilde{P}'_\theta$) adapted to the Brownian motion simulation technique [15]. AMA has been validated by comparison to a 1D analytical model in transient regime [15] and to the axi-symmetrical model presented above in steady state [23].

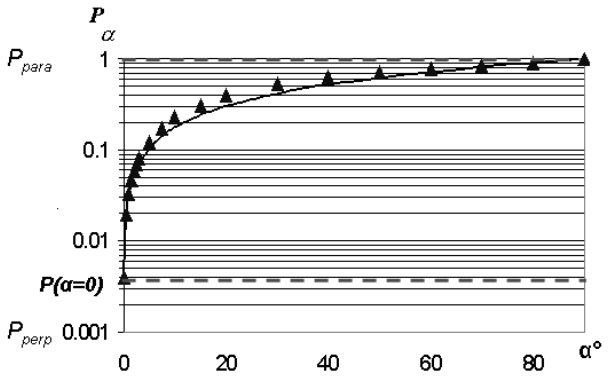

Figure 8. Effective sticking probability of a stack as a function of its relative orientation to the surface

In the literature, the actual gasification rates of parallel and perpendicular direction are never quantitatively reported. In the scope of reproducing larger scale behavior and to progress in turbostratic carbon modeling before carrying out difficult experiments, the parallel to perpendicular ratio has been fixed to 1000. Then, the Damköhler number has been taken very low. Indeed, this assumption seems to be correct in the field of the considered applications (see subsection 4.1). The effective sticking probability, P_α, is reported as a function of graphene stack orientation to surface α, on figure 8, where the sticking probabilities have been normalized. The filled triangles

are the simulation points. The curve is a representation of an approximation of the numerical result; this approximation ($P_\alpha = a + b\,\alpha^{0.8}$, where a and b are two constants) is used in the following to compute the next change of scale. Note that the lower sticking probability, $P_{(\alpha=0)}$, is no longer $P_\perp$. This fact is due to the ability of the random walk code to simulate random events. In particular, the pitting of a graphene plane followed by a pit extension in the perpendicular direction is taken into account in effective reactivity evaluation. This phenomenon, experimentally observed [27] and already simulated in 2D [28], is simulated in 3D in this work (figure 9). Thus, the effective sticking event in perpendicular direction is increased by this phenomenon.

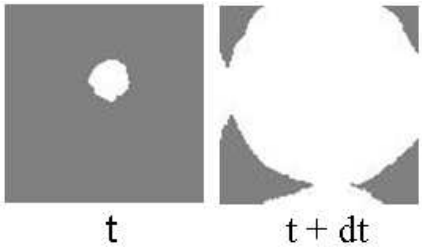

Figure 9. Pitting on a graphene stack for $\alpha = 0$: pit growth. Surface top view.

4.2.3. Second change of scale: graphene stack to material

In the case of EDM3 poly-crystalline graphite, the graphene stack can be assimilated to the grain. Two poly-crystalline graphites have been randomly processed following the EDM3 gaussian law of grain repartition (see subsection 3.2). The first one is an ideal graphite : the grains are well connected (see figure 10). In a more realistic way, the second one includes a pitch-based matrix joining the grains (see figure 11). The matrix is a homogeneous material. Its reactivity value is taken equal to the arithmetic average of P_α. Each grain orientation is chosen by a random process according to a normal law for the angle; on the figure, the gray scale values span from black ($\alpha = 0°$) to white ($\alpha = 90°$). These materials are globally isotropic. The sticking probability law P_α is used to simulate the graphite ablation. A steady state regime, with a stabilized surface roughness height, is obtained after the ablation of approximatively ten grain levels. The surface roughness is linked to material structure. It is of the order of magnitude of the grain size for the chosen reactivity ratio between perpendicular and parallel directions. Two qualitative results tends to validate the model. First, the surface roughness simulation is in correct agreement with observations. The agreement may be improved with a more realistic modeling of the material. Second, the sensitivity of the model to grain size (or graphene plane extension) is in agreement with the experimental results of the literature (see section 2).

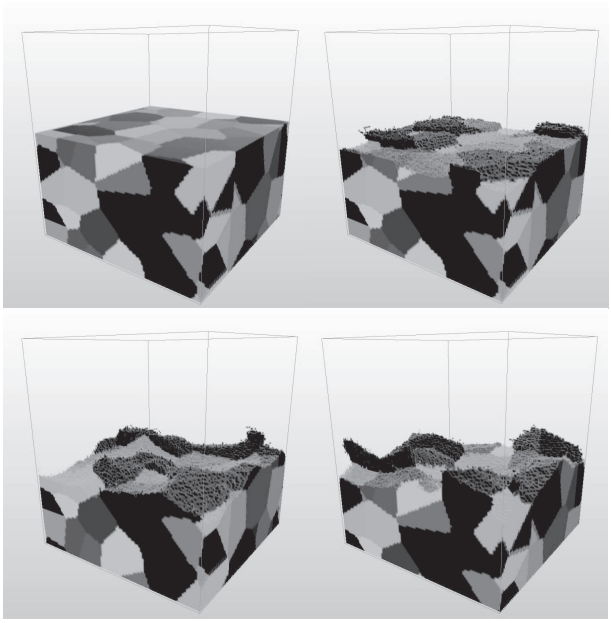

Figure 10. Simulation of the surface evolution of an ideal poly-crystalline graphite during ablation

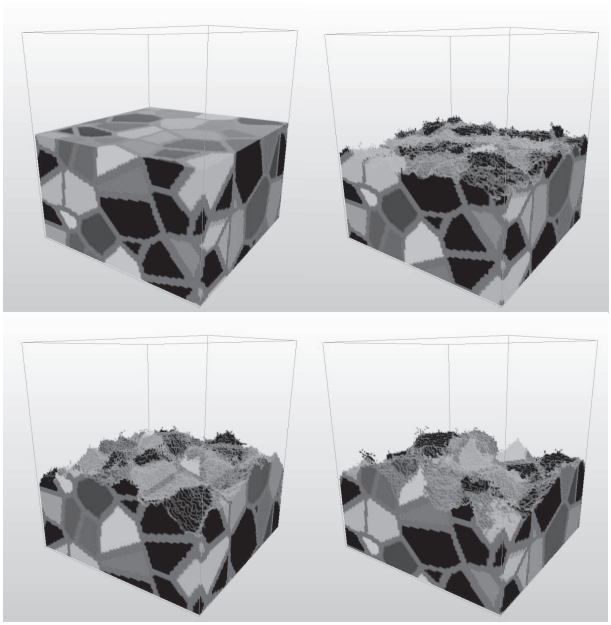

Figure 11. Simulation of the surface evolution of a poly-crystalline graphite with grain joint during ablation

5. CONCLUSION AND OUTLOOKS

In this work, the origin and development of surface roughness on a 3D-C/C composite and on a poly-crystalline graphite during ablation are tackled. First, the link between turbostratic carbons structure and the ablation behavior of carbon-based materials is analyzed : it

underlies the overall ablation phenomena. Second, using as a reference arc-jet test and oxidation test samples, multi-scale roughness is observed, classified and briefly analyzed for these two materials. Then the focus is set on the well-known "needle clusters" roughness features which develop on emerging bundles of C/C composites. A simple heterogeneous reaction/diffusion model is presented and the results of an analytical solution in steady state are summarized. The model, which has been experimentally validated, opens a complete understanding of the material behavior at this scale. However, at lower scales the anisotropic structure has a strong effect on surface roughness and material behavior. To progress in this study, the poly-crystalline graphite is used as a model material.

To model the ablation behavior of the poly-crystalline graphite, which is a particular turbostratic carbon, an anisotropic reactivity is included in the model. It takes into account its turbostratic structure. The starting point of the model is the graphene plane. An interpretation of graphene reactivity as a function of its parallel and perpendicular reactivities is proposed. Then, two successive changes of scales following the material structure are processed (graphene plane $\Rightarrow$ graphene stack (or grain) $\Rightarrow$ material). Those changes of scales are done using an homemade simulation code, which handles efficiently anisotropic reactivities. At each scale, the sensitivity of the model to the study parameters are consistent with literature data. At the last scale, simulation results can be compared to SEM and CMT observations: a correct qualitative agreement is obtained. The model could be improved by a better description of the material. Despite a lack of nano-scale feeding data for a quantitative validation, results are promising, since the proposed model can qualitatively explain roughness development on graphite.

To progress in the turbostratic carbon modeling, experimental studies have to be carry out to determine graphene plane reactivities.

At macroscopic scale, the model of C/C ablation should include heat transfer and advection close to the wall, as well as the anisotropic reactivity of C fibers.

ACKNOWLEDGMENTS

The authors wish to thank CNRS and CEA for Ph. D. grant to J. Lachaud.

REFERENCES

[1] J. Couzi, J. de Winne, and B. Leroy. Improvements in ablation predictions for reentry vehicle nosetip. In *Proceedings of the third European symposium on aerothermodynamics for space vehicles*, pages 493–499, ESA, Noordwijk, The Nederlands, 24-26 November 1998.

[2] G. Duffa, G. L. Vignoles, J.-M. Goyhénèche, and Y. Aspa. Ablation of C/C composites : investigation of roughness set-up from heterogeneous reactions. *International Journal of Heat and Mass Transfer*, 48(16):3387–3401, June 2005.

[3] L. M. Manocha and E. Fitzer. *Carbon reinforcement and C/C composites*. Springer, 1998.

[4] M. R. Wool. Summary of experimental and analytical results. Technical Report SAMSO-TR-74-86, Passive Nosetip Technology Program (PANT), January 1975.

[5] J. A. Keenan and G. V. Candler. Simulation of ablation in earth atmospheric entry. In AIAA Paper, editor, *AIAA 28th Thermophysics conference*, volume 93, Orlando, FL, July 1993.

[6] C. Sauder. *Relation microstructure/propriétés à haute température dans les fibres et matrices de carbone*. PhD thesis n°2477, Université Bordeaux 1, 2001.

[7] X. Bourrat. *Sciences of carbon materials*, chapter 1. Structure in carbons and carbon artifacts, pages 1–97. Universitad de Alicante, 2000.

[8] J-M. Vallerot, X. Bourrat, A. Mouchon, and G. Chollon. Quantitative structural and textural assessment of laminar pyrocarbons through raman spectroscopy, electron diffraction and few other techniques. *Carbon*, 44(9):1833–1844, 2006.

[9] A. Oberlin, J. Goma, and J. N. Rouzaud. Techniques d'étude des structures et texture (microtextures) des matériaux carbonés. *J. Chimie Physique*, 81(11/12):701–710, 1984.

[10] J. B. Donnet. Structure and reactivity of carbons: from carbon black to carbon composites. In *15th Biennal conference on carbon*, Philadelphia, PE, June 1981.

[11] E. J. Hippo. The role of active sites in the inhibition of gas-carbon reactions. *Carbon*, 27(5):689–695, 1989.

[12] G. H. Hennig. Anisotropic reactivities of graphite - I. Reaction of ozone and graphite. *Carbon*, 3(2):107–108, 1965.

[13] P. Chantrenne and S. Volz. Introduction à la dynamique moléculaire. *Techniques de l'ingénieur*, BE(8290):1–20, 2002.

[14] P. Delhaes. *Le carbone dans tous ses états*, chapter 1. Le polymorphisme des solides carbones, pages 1–118. Gordon and Breach Science Publishers, 1997.

[15] J. Lachaud, G. L. Vignoles, J. M. Goyhénèche, and J. F. Epherre. Ablation in C/C composites: microscopic observations and 3D numerical simulation of surface roughness evolution. In L. P. Cook, editor, *Thermochemistry and Metrology of Interfaces*, volume 191 of *Ceramic Transactions*, page 12. American Ceramic Society, 2006.

[16] D. Cho, J. Y. Lee, and B. I. Yoon. Microscopic observations of the ablation behaviours of carbon fibre/phenolic composites. *Journal of materials science letters*, 12:1894–1896, 1993.

[17] E. Duvivier. *Cinétique d'oxydation d'un composite carbone/carbone et influence sur le comportement mécanique*. PhD thesis n°1692, Université de Bordeaux I, 1997.

[18] D. Cho and B. I. Yoon. Microstructural interpretation of the effect of various matrices on the ablation properties of carbon-fiber-reinforced composites. *Composites science and technology*, 61:271–280, 2001.

[19] J. C. Han, X. D. He, and S. Y. Du. Oxidation and ablation of 3D carbon-carbon composite at up to 3000°C. *Carbon*, 33(4):473–478, 1995.

[20] Y.-J. Lee and H. J. Joo. Investigation on ablation behavior of CFRC composites prepared at different pressure. *Composites: Part A*, 35:1285–1290, 2004.

[21] E. Dourthe, A. Cosculluela, and D. Rousselle. Etude des propriétés d'ablation des graphites à l'aide d'une torche à plasma. Technical report, Rapport CEA-DAM CEB.III-DETN Service matériaux avancés, 1995.

[22] G. Vignoles, Y. Aspa, J. Lachaud, G. Duffa, J. M. Goyheneche, J. F. Epherre, N. T. H. Nguyen-Bui, M. Quintard, and B. Dubroca. Multiscale study of ablation in carbon/carbon composites : Surface roughness evolution and possible physicochemical causes. In *ESA Workshop on Ablation, ESTEC*, Noordwijk, The Netherlands, 13 Oct 2005.

[23] J. Lachaud, Y. Aspa, G. Vignoles, and G. Bourget. Experimental characterization and 3d modelling of carbon/carbon composites oxidation : role of the interphase. *Submitted to* 12^{th} *European Conference on Composite Materials*, Biarritz, France, 1-3 September 2006.

[24] N. Bertrand, J. Lachaud, G. Bourget, F. Rebillat, and G. L. Vignoles. Identification of intrinsic carbon fiber oxidation kinetics from experimental data and CFD modeling. *Submitted to* 12^{th} *European Conference on Composite Materials*, Biarritz, France, 1-3 September 2006.

[25] G. L. Vignoles. Modelling binary, Knudsen, and transition regime diffusion inside complex porous media. *J. Phys. IV France*, C5:159–166, 1995.

[26] S. Torquato and I. Kim. Efficient simulation technique to compute effective properties of heterogeneous media. *Appl. Phys. Lett.*, 55:1847–1849, 1989.

[27] J. R. Hahn. Kinetic study of graphite oxidation along two lattice directions. *Carbon*, 43:1506–1511, 2005.

[28] F. Stevens and T. P Beebe. Computer modeling of graphite oxidation: differences between monolayer and multilayer etching. *Computers and Chemistry*, 23:175–183, 1999.